

# Phosphodiesterase-5A (PDE5A) is localized to the endothelial caveolae and modulates NOS3 activity

Milena A. Gebska<sup>1,2</sup>, Blake K. Stevenson<sup>1</sup>, Anna R. Hemnes<sup>3</sup>, Trinity J. Bivalacqua<sup>4</sup>, Azeb Haile<sup>1</sup>, Geoffrey G. Hesketh<sup>1</sup>, Christopher I. Murray<sup>1</sup>, Ari L. Zaiman<sup>5</sup>, Marc K. Halushka<sup>6</sup>, Nispa Krongkaew<sup>6</sup>, Travis D. Strong<sup>5</sup>, Carol A. Cooke<sup>7</sup>, Hazim El-Haddad<sup>1</sup>, Rubin M. Tuder<sup>10</sup>, Dan E. Berkowitz<sup>8</sup>, and Hunter C. Champion<sup>1,4,9\*</sup>

<sup>1</sup>Division of Cardiology, Department of Medicine, Johns Hopkins University School of Medicine, Rutland Avenue, Baltimore, MD 21205, USA; <sup>2</sup>Division of Cardiovascular Diseases, Department of Medicine, University of Iowa, Hospitals and Clinics, 200 Hawkins Drive, Iowa City, IA 52242, USA; <sup>3</sup>Division of Pulmonary, Allergy, and Critical Care Medicine, Vanderbilt University School of Medicine, Nashville, TN, USA; <sup>4</sup>The James Buchanan Brady Urological Institute, Department of Urology, Johns Hopkins Medical Institutions, 600 North Wolfe St., Marburg 143, Baltimore, MD 21287, USA; <sup>5</sup>Division of Pulmonary, Allergy, and Critical Care Medicine, Johns Hopkins University School of Medicine, Rutland Avenue, Baltimore, MD 21205, USA; <sup>6</sup>Department of Pathology, Department of Medicine, Johns Hopkins Medical Institutions, Ross RM 632L, 720 Rutland Avenue, Baltimore, MD 21205, USA; <sup>7</sup>Department of Cell Biology and Imaging, Johns Hopkins University School of Medicine, 725 N. Wolfe St., Baltimore, MD 21205, USA; <sup>8</sup>Department of Anaesthesiology and Critical Care Medicine, Johns Hopkins Medical Institutions, 600 N. Wolfe St., Baltimore, MD 21287, USA; <sup>9</sup>Division of Pulmonary, Allergy, and Critical Care Medicine, Department of Medicine, Vascular Medicine Institute, University of Pittsburgh School of Medicine, NW628 Montefiore Hospital, 3459 Fifth Avenue, Pittsburgh, PA 15260, USA; and <sup>10</sup>Program in Translational Lung Research, University of Colorado Denver, 13001 E. 17th Place, Aurora, CO 80045, USA

Received 25 March 2010; revised 20 December 2010; accepted 22 December 2010; online publish-ahead-of-print 18 March 2011

Time for primary review: 19 days

## Aims

It has been well demonstrated that phosphodiesterase-5A (PDE5A) is expressed in smooth muscle cells and plays an important role in regulation of vascular tone. The role of endothelial PDE5A, however, has not been yet characterized. The present study was undertaken to determine the presence, localization, and potential physiologic significance of PDE5A within vascular endothelial cells.

## Methods and results

We demonstrate primary location of human, mouse, and bovine endothelial PDE5A at or near caveolae. We found that the spatial localization of PDE5A at the level of caveolin-rich lipid rafts allows for a feedback loop between endothelial PDE5A and nitric oxide synthase (NOS3). Treatment of human endothelium with PDE5A inhibitors resulted in a significant increase in NOS3 activity, whereas overexpression of PDE5A using an adenoviral vector, both *in vivo* and in cell culture, resulted in decreased NOS3 activity and endothelium-dependent vasodilation. The molecular mechanism responsible for these interactions is primarily regulated by cGMP-dependent second messenger. PDE5A overexpression also resulted in a significant decrease in protein kinase 1 (PKG1) activity. Overexpression of PKG1 rapidly activated NOS3, whereas silencing of the PKG1 gene with siRNA inhibited both NOS3 phosphorylation (S1179) and activity, indicating a novel role for PKG1 in direct regulation of NOS3.

## Conclusion

Our data collectively suggest another target for PDE5A inhibition in endothelial dysfunction and provide another physiologic significance for PDE5A in the modulation of endothelial-dependent flow-mediated vasodilation. Using both *in vitro* and *in vivo* models, as well as human data, we show that inhibition of endothelial PDE5A improves endothelial function.

## Keywords

PDE5A • Phosphodiesterase • Endothelial cells • Lipid rafts • Caveolin-1 • Sildenafil • NOS3 • cGMP • Adenoviral transfection • Primary human endothelial cells • Signalling pathway • Pulmonary circulation

## 1. Introduction

In the vasculature, the nitric oxide/cyclic guanosine-3',5'-monophosphate/protein kinase G (NO/cGMP/PKG) signalling

pathway is the fundamental endogenous vasodilator system known; however, its downstream pathway is still not well understood.<sup>1</sup> Historically, it has been believed that smooth muscle cells (SMCs) are the only reservoir of the phosphodiesterase-5A (PDE5A).

\* Corresponding author. Tel: +1 412 692 2210; fax: +1 412 692 2260, E-mail: championhc@upmc.edu

Recent studies demonstrate PDE5A expression/activity in other cell types, including cardiac myocytes<sup>2</sup> and vascular endothelial cells (ECs).<sup>3–5</sup> However, its exact location or functional role in endothelium has not been fully characterized.

Activation of soluble guanylyl cyclase by NO leads to an increased synthesis of the second messenger, cGMP, and stimulation of cGMP-dependent PKG. Mammalian PKG exists in two major forms: PKG1, a soluble enzyme consisting of  $\alpha$  and  $\beta$  isoforms derived from alternative splicing from one gene, and PKG2, a myristoylated, membrane-associated form derived from a second gene.<sup>6</sup> Recent *in vitro* and *in vivo* studies on knockout mice identified SMC-derived PKG1 as a major mediator of cGMP signalling in the cardiovascular system. Little is known, however, on the role of endothelium-derived PKG in regulation of NO-mediated vasodilatation.

The body of current literature provides evidence that most of the signalling molecules of the NO cascade, including NOS,<sup>7,8</sup> sGC, PKG1, and PKA,<sup>9,10</sup> localize to the subendothelial caveolae. Here we show that PDE5A is also localized at the level of caveolin-rich lipid rafts within vascular endothelium. The spatial localization led us to hypothesize that PDE5A may reciprocally regulate nitric oxide synthase (NOS3) activity. Until now, no direct link between endothelial PDE5A and NOS3 activity has been described in literature. We used both *in vitro* and *in vivo* models as well as human data to provide evidence that inhibition of endothelial PDE5A improves endothelial function, thus demonstrating a potential for PDE5A inhibitor therapy in human disease. Finally, the fact that we found PDE5A at the level of caveolar compartment provides a novel concept of a traditional NO/cGMP/PDE5A signalling pathway to be fully functional in vascular endothelium, independently on SMCs.

## 2. Methods

All animal protocols were approved by the Animal Care and Use Committee, Johns Hopkins University; the investigation confirmed with the Guide for the Care and Use of Laboratory Animals published by the US National Institutes of Health (NIH Publication No. 85-23, revised 1996). All experiments involving human cells were conducted in full accordance with the US National Institutes of Health guidelines and Declaration of Helsinki.

### 2.1 Cell culture

After obtaining Ethical Committee approval, human aortic (HAECs) and human coronary artery (HCAECs) endothelial cells were isolated from samples retrieved from explanted hearts removed for orthotopic cardiac transplantation, as previously described.<sup>11</sup> Briefly, under sterile conditions, vessels were cut into 3–4 mm sections and placed for 2 days in fully supplemented ECM Medium (ScienCell Research Laboratories). After reaching ~85% confluence, ECs were purified using CD31 Dynabeads (Invitrogen Corporation). The culture cellular composition was determined by their morphology and immunofluorescence. At least 98% of the cells were von Willebrand factor (vWF) (Santa Cruz Biotechnology)-positive.<sup>12</sup> Monoclonal antibody AS02 (Calbiochem-EMD Chemicals) was used to determine population of fibroblasts.<sup>13</sup>

Primary mouse aortic (MAECs) and pulmonary (MPAECs) endothelial cells were harvested, as described earlier.<sup>14</sup> Cells were uniformly positive for Factor VIII (Innovex). Isolation of murine MPAECs was performed as previously described<sup>15</sup> using anti-endoglin (CD-106) antibodies (BD Transduction Lab), a mini-MACS separation unit (Miltenyi Biotec), and flow cytometry. Labelled cells were incubated with MACS Magnetic Goat Anti-mouse IgG (H1L) (Miltenyi Biotec) MicroBeads and

Streptavidin (Miltenyi Biotec) MicroBeads, and then separated using a high-gradient magnetic separation column (Miltenyi Biotec).

Bovine aortic (BAECs), human umbilical vein (HUVECs), and human pulmonary artery (HPAECs) endothelial cells were all purchased from Cambrex<sup>®</sup> (Cambrex Corporation).

### 2.2 Preparation of raft-enriched membrane fractions using detergent resistance method

Isolation of endothelial caveolin-1 was carried out according to earlier described methods.<sup>16</sup> Briefly, confluent monolayers of cultured BAECs were washed with phosphate-buffered saline (PBS) and subjected to a small amount of protein inhibitor cocktail in TKMT buffer (50 mM Tris, 25 mM KCl, 5 mM MgCl<sub>2</sub>, 1 mM ethylenediaminetetraacetic acid) containing 1% Triton X-100. After 20 min, cells were scraped and sonicated using PRO-200. Cell lysates (0.5 mL) were subsequently mixed with equal amount of 80% sucrose/TKMT buffer, on top of which 38 and 5% sucrose/TKMT were layered, and centrifuged at 285 000 g for 18 h using Beckman SW1T1 swinging bucket rotor at 4°C in a Beckman Optima<sup>™</sup> XL-100K Ultracentrifuge. Twelve fractions (1 mL each) were collected from the top of each gradient and placed on ice. Then, 150  $\mu$ L of 15% of ice-cold trichloroacetic acid (TCA) was added to each aliquot. Suspension aliquots were then washed with acetone, and pellets were re-suspended in 5% sodium dodecyl sulphate (SDS)/PBS buffer. Protein quantitation was performed using Bradford's method.

### 2.3 Quantitative polymerase chain reaction

Total RNA was isolated using RNeasy Kit (Qiagen), DNase treated (Ambion), and reverse-transcribed using Superscript II (Life Technologies). Polymerase chain reactions (PCR) were performed in a GeneAmp 7900 sequence detection system (Applied Biosystems) using SYBR green PCR master mix, according to the standard protocol. To amplify specific gene products, the following intron-spanning primers were used: sense, 5'-CCTTGTGCAGAACTCCAGA-3'; antisense, 5'-TCCGTTGTTGAA TAGG CCAG-3'. Mouse glyceraldehyde-3-phosphate dehydrogenase (GAPDH) was co-amplified as an internal control, using the following primer sequences: GAPDH sense: 5'-CATCCATCTTCCAGGA GCG-3'; antisense: 5'-GAGGGGCCAATCCACAG TCTTC-3'. Standard curves were performed using GAPDH to ensure appropriate RNA loading per sample.

### 2.4 PDE5A and PDE1A siRNA transfection

PDE5A and PDE1A (NP\_001003683.1) siRNAs were designed and synthesized by Dharmacon with the sequences CCTTGTGCAGAACTT CCAG and CCACATAGGAAGAAGTTTCG, respectively.

### 2.5 PKG1 $\alpha$ $\beta$ siRNA transfection

The catalytic domain sequence of bovine PKG1 (GenBank Accession No. X16086), base pairs 999–2016, was used as the template to design the siRNA that targets PKG1 $\alpha$  and  $\beta$  transcripts. siRNAs were synthesized by Qiagen, and the double-stranded small interfering RNA (ds-siRNA) that we used to silence PKG, was generated as previously described<sup>17</sup> by annealing the two strands, namely sense, r(CCU UCU UUA UCA UCA GUA A)dTdT, and antisense, r(UUA CUG AUG AUA AAG AAG G)dTdG.

### 2.6 Transfection with recombinant adenovirus

PDE5A-recombinant adenovirus (AdPDE5A; titre  $1 \times 10^9$  pfu/mL) was obtained from Vector Biolab<sup>®</sup> per special request. Adenovirus encoding  $\beta$ -galactosidase (Ad $\beta$ gal) and recombinant NOS3 adenovirus (Ad5CMV $\beta$ -NOS, titre  $1 \times 10^{10}$  pfu/mL) were purchased from the Gene Transfer Vector Core, University of Iowa. The calculated amount of virus was diluted in a Dulbecco's modified Eagle medium without fetal calf serum

in order to achieve multiplicity of infection (MOI) between 30 and 125. Viral vectors were driven by CMV promoter in cell culture applications and Tie2 promoter in vascular experiments requiring targeted transfection of vascular endothelium.

## 2.7 Transfection with recombinant PKG1 $\alpha$ virus

DsRed monomer was cloned by PCR from pDsRed-N1 (Clontech) vector using a forward primer (5'-GGATTTAAACTCGAGCGCCACCATGGACAACACCGAG-3') and a reverse primer (5'-TCCTTTAACTACTGGGAGCCGGAGTGGC-3'). The PCR product was then inserted into a shuttle vector using the TA Cloning Kit (Invitrogen Corporation) following the manufacturer's protocol. *EcoRI* was used to subclone DsRed monomer into Adenovirus serotype V vector, driven by a CMV promoter. PCR was again performed using a forward primer (5'-GAATTCGGATCCGCCACCATGGACTACAAAGACCATGACGGTGATTATAAAGATCATGACATCGATTACAAGGATGACGATGACAAGATGAGCGAGCTAGAGGAAGAC-3') and a reverse primer (5'-GAATTCCTTATGGATCCATGAAGTCTATATCCCATCCTGAG-3') to add a 3 $\times$  Flag at the N terminus and to delete the stop codon at the C terminus of human PKG1 $\alpha$  coding sequence. *BamHI* was further used to subclone Flag-tagged PKG1 $\alpha$  into the Ad-DsRed vector described above; it was inserted at the N terminus of DsRed monomer and formed an in-frame fusion protein. All the PCR products and in-frame junction were sequenced. Adenovirus was produced in 293 cells after recombination with the virus DNA and further purified using CsCl method. Final concentrated virus was dialyzed in Tris-MgCl buffer and the titre is  $6.36 \times 10^9$  pfu/mL. The cells were transfected for 24 or 48 h, depending on experimental requirements.

## 2.8 Protein activity assays

cGMP-dependent PDE activity assays are given as follows: (1) Phosphodiesterase [ $^3\text{H}$ ]cGMP Scintillation Proximity Enzyme Immunoassay (Amersham Biosciences); (2) Cyclic Nucleotide Phosphodiesterase Assay (Biomol International); (3) IMAP-FP Phosphodiesterase Evaluation Assay (Molecular Devices Corporation), using a Microplate SpectraMax M5 (Molecular Devices Corporation), excitation/emission 485 nm/525 nm filter set, auto cut-off 515 nm.

NOS3 activity assays are given as follows: (1) L-[ $^{14}\text{C}$ ]arginine-to-L-[ $^{14}\text{C}$ ]citrulline conversion using the NOSdetect Assay Kit (Cayman Chemical), where enzyme activity was expressed as L-citrulline production in  $\text{pmol min}^{-1} \text{mg protein}^{-1}$ ; (2) Nitrate/Nitrite Colorimetric Assay (Cayman Chemical); (3) Fluorimetric DAF2 using Cell-Associated NOS Detection Kit (Sigma-Aldrich); DAF2-DA fluorescence was quantified using MetaMorph software.

cGMP-dependent PKG activity was assayed by colorimetric analysis (CycLex; MBL International Corporation, Woburn, MA, USA) from EC extracts according to the manufacturer's instructions, as previously described.<sup>18</sup> Total endothelial PKG activity is expressed as relative light units (arbitrary units) per mg of protein. Total PKG activity was expressed as a percentage of the control.

## 2.9 Western blotting and immunoprecipitation analysis

The blots were probed with the following primary antibodies: PDE5A, P-eNOS(S1177); P-PDE5A(S92) antibody was a gift from D. Koesling, Institut für Pharmakologie und Toxikologie, Bochum, Germany; PKG1 $\beta$  (Stressgen Bioreagents); PKG1 $\alpha$  antibody was a gift from Dr Michael E. Mendelsohn, Molecular Cardiology Research Institute, Tufts-New England Medical Center, Boston, MA, USA; NOS3 polyclonal IgG (Santa Cruz Biotechnology); P-eNOS(S1179) (Invitrogen Corporation), Caveolin-1 monoclonal IgG1 (BD Biosciences), sGC1 $\alpha$  (Sigma-Aldrich). For PDE5 immunoprecipitation, PDE5 antibody (a gift from S.S. Visweswariah, Indian Institute of Science, Bangalore, India) and Pierce Seize X

Immunoprecipitation Kit were used. The immunopositive bands were visualized by using SuperSignal<sup>®</sup> Chemiluminescent Kit (Pierce). Antibody Stripping Buffer (FabGennix, Inc.) was used for re-probing the membranes. The intensities of the resulting bands were quantified by using Software Image J 1.43s NIH.

## 2.10 Confocal and electron microscopy

Cells were fixed and probed with the appropriate primary antibody tagged to PDE5A and Alexa red and NOS3 tagged to Alexa green (Alexa Fluor 488 and 546 IgG, respectively; Molecular Probes), and mounted with Vectashield DAPI mounting medium (Vector Laboratories, Inc.). All images were acquired within 1 h using Zeiss LSM510 confocal microscope equipped with a 20 $\times$ , 63 $\times$ , or 100 $\times$  C-Apochromat 1.2 NA water immersion objective lens. Images were processed using Adobe Photoshop<sup>®</sup> software (Adobe Systems).

Confluent ECs were processed as described previously.<sup>19</sup> Cell pellets were fixed in 4% formaldehyde in 0.1 M sodium cacodylate supplemented with 3% sucrose and 3 mM CaCl<sub>2</sub> and cryoprotected in 2.3 M sucrose overnight, in polyvinylpyrrolidone (Sigma) and frozen in liquid nitrogen. Ultrathin sections were cut on a Leica Ultracut UCT microtome, and sections were placed on formvar-coated nickel 200 mesh hexagonal grids. The sections were incubated in primary antibody for either 1 h at room temperature or overnight at 4°C at a concentration of 10  $\mu\text{g/mL}$ . Primary antibodies were detected 6 nm colloidal goat anti-rabbit (Jackson Immuno-Research) diluted 1:20 in PBS for 1 h. Final contrasting of the sections was done by incubating them in 2% methyl cellulose (Sigma) and 0.3% uranyl acetate (Ted Pella) for 10 min at 4°C. All sections were viewed with a Hitachi 7600 TEM at an accelerating voltage of 80 kV. Images were taken with an AMT digital camera.

## 2.11 Physiological studies

### 2.11.1 *In vivo* gene transfer technique

Details of the transfection procedure have been previously reported by our laboratory.<sup>15,20,21</sup> Male C57BL/6 mice (20–30 g) were anesthetized with isoflurane (2%), endotracheally intubated, and ventilated on a thermoregulated table at 37°C. The left external jugular vein was dissected and cannulated. Mice were cooled with a water jacket to a core temperature of 19–21°C (heart rate  $\approx$  100 b.p.m.), the distal pulmonary artery (PA) was clamped, and Ad $\beta$ gal or AdVTie2PDE5A injected IV (30  $\mu\text{L}$ ). The PA clamp was released after 5 min, inotropic and/or pacing support provided as needed, the mouse was warmed to 37°C for 30–40 min, and the chest closed. This method of gene transfer yields broadly distributed transfection throughout the pulmonary vasculature, with approximately 60% of individual EC being transfected (based on the analysis of  $\beta$ -gal expression).<sup>15</sup> Tie2-based gene expression peaks at 3–4 days and gradually declines thereafter returning to baseline over the ensuing 1–2 weeks. Therefore, we performed all functional analyses 3–4 days after gene transfer.

### 2.11.2 Isolated mouse PA segments

Post-transfection (see Section 2.11.1), a second-order PA was isolated, and 2–3 mm vascular rings were subjected to further testing. Vascular segments were secured within Halpern–Mulvany myography chamber (Living Systems Instrumentation, Burlington, VT, USA). Luminal diameters were monitored on the computer screen under basal conditions and in the presence or absence of vasoconstrictors/vasodilators. The resting tension–internal circumference relation was determined for each segment according to Mulvany and Halpern.<sup>22</sup>

## 2.12 Statistical analysis

Data are reported as mean  $\pm$  SEM. Differences between multiple experimental groups were compared by analysis of variance. Analysis between two groups was performed by t-test (paired or unpaired as appropriate).

Prism 5.0 and Microsoft Excel programs were used to analyse and graphically represent data.

### 3. Results

#### 3.1 PDE5A gene is actively expressed in vascular endothelium and its primary location is at the level of caveolin-rich lipid rafts

Gene expression of PDE5A-mRNA in vascular ECs was studied using quantitative PCR (qPCR). When data were normalized for GAPDH, a significant and comparable expression of mRNA was found in all cell types (data not shown). Immunoblotting for PDE5A derived from

various vascular ECs demonstrated a prominent band at 100 kDa in bovine (BAEC) and human tissues, as indicated in *Figure 1A*.

We next measured total cGMP-dependent phosphodiesterase (PDE) activity in order to characterize PDE5A activity. As depicted in *Figure 1B*, when MPAECs were treated with two selective PDE5A inhibitors sildenafil (sild) and tadalafil (tad) at 1  $\mu$ M/48 h, approximately 59 and 49% of the total cGMP-dependent PDE, respectively, was due to PDE5A activity (as represented by the black bars; *Figure 1B*). Confirmation using the same assay was performed after transfection of siRNA against two major cGMP-dependent endothelial phosphodiesterases (PDE5A and PDE1A) for 36 h. Approximately 40% of cGMP-dependent PDE activity in vascular endothelium was attributable to PDE5A, whereas PDE1A contributed  $\sim$ 25% (as depicted by the values shown in the black bars of *Figure 1B*). These data suggest that  $\sim$ 65% of the total cGMP-dependent PDE activity in the mouse

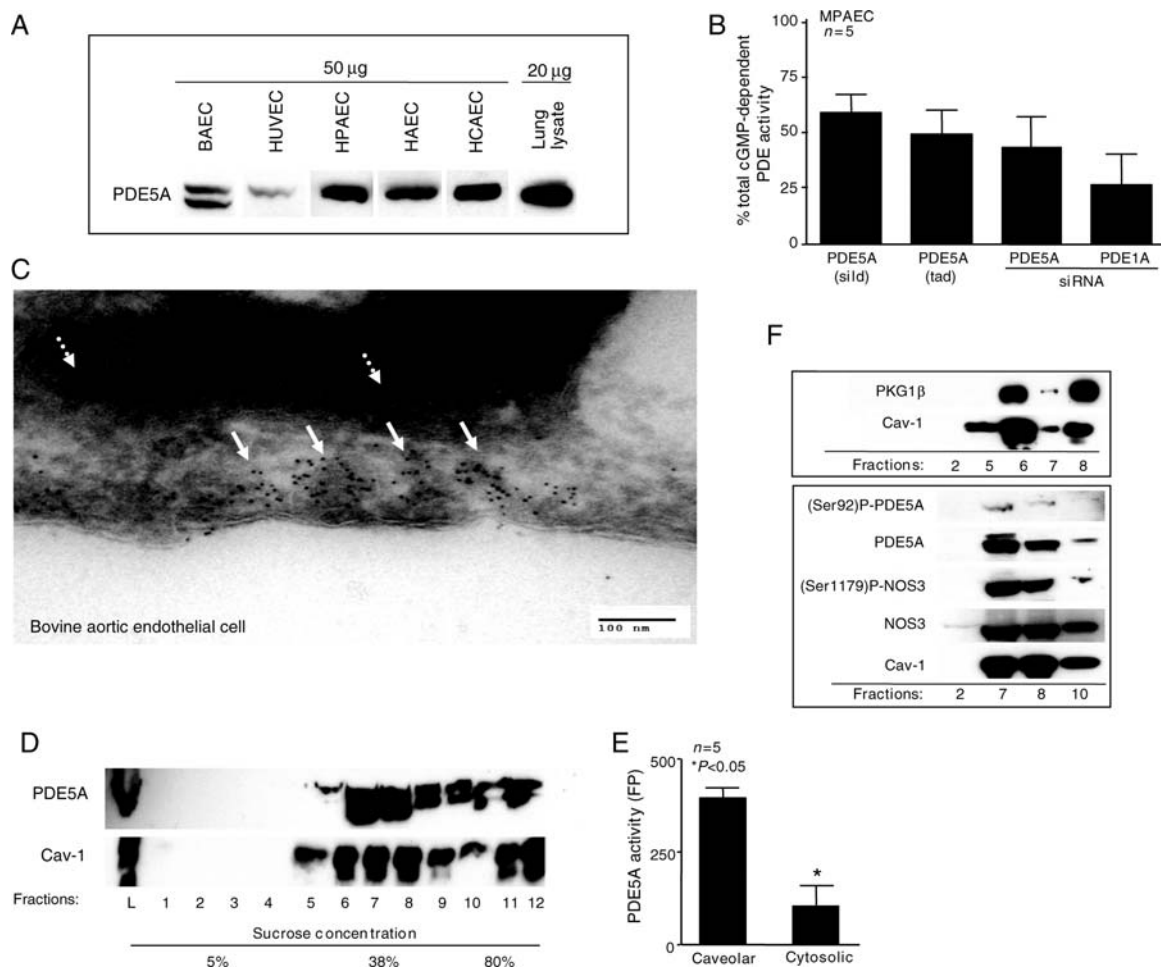


**Figure 1** PDE5A gene is actively expressed in vascular ECs and its primary location is at the level of caveolae. (A) Representative immunoblot of PDE5A expression in cultured BAECs, HUVECs, HPAECs, HAECs and HCAECs. The amount of protein is marked on top of the blot. A total mouse lung lysate served as a positive control. (B) Relative cGMP-dependent PDE activity in the presence of sildenafil (sild), tadalafil (tad), or following transfection of MPAECs with siRNA against PDE5A or PDE1A, expressed as a final percentage of untreated control ( $n = 5$ ,  $*P < 0.05$ ,  $\pm$  SEM). The bars denote the % of the total cGMP-dependent PDE activity as it relates to PDE5A (first three bars) and PDE1A (last bar). (C) Electron micrograph showing PDE5A to be heavily concentrated within the subendothelial caveolae (white solid arrows) of cultured BAECs. White interrupted arrows indicate distribution of PDE5A in cytosol. (D) Representative immunoblot of the whole BAEC cell lysates (L) and cellular fractionation, based on sucrose density gradients, for Cav-1 and PDE5A. (E) Radiolabelled PDE activity of PDE5A following IP within caveolar and cytosolic compartments ( $*P < 0.005$ ,  $\pm$  SEM,  $n = 5$ ). (F) Immunoblots for NOS3, P-NOS3(S1179), PDE5A, P-PDE5A(S92), Cav-1, and PKG1 $\beta$  in selected cytosolic and sub-cellular BAEC lipid-enriched fractions, as indicated.

pulmonary endothelium is due to PDE5A and PDE1A. The remaining 35% of cGMP-dependent PDE activity is most likely due to the presence PDE5A isoforms that were not detected by our method (e.g. PDE5A1, PDE5A2, or PDE5A3). IMBX, a non-specific PDE inhibitor, blocked about 85% of cGMP-dependent PDE, suggesting that activity of endothelial PDE8 and PDE9 is about 15% (data not shown).

We next sought to determine the subcellular localization of endothelial PDE5A. Confocal microscopy and staining with antibodies against vWF confirmed primary human EC culture purity to be >98% (data not shown). We observed a diffuse staining pattern with antibody to PDE5A in all tested cell types and in cultured human coronary ECs. Given the spatial localization of NOS3 within caveolae,<sup>8</sup> as well as immunohistochemical evidence for sGC and PKG at or near caveolae,<sup>9,10</sup> we hypothesized that perhaps PDE5A is also present at or near caveolae, as a mechanism to regulate cGMP/PKG activity. Immuno-gold 6 nm particles showed PDE5A to be heavily concentrated within the subendothelial invaginations of BAECs (Figure 1C, white arrows). A scattered distribution of PDE5A

was also seen in cytosol (Figure 1C, white interrupted arrows). These findings were further supported by immunoblotting of subcellular fractionation of BAECs showing co-expression of caveolin-1 (Cav-1) and PDE5A (Figure 1D–F), which correlated with significantly increased cGMP-dependent PDE activity ( $P < 0.05$ ) following PDE5A immunoprecipitation (Figure 1E). In addition, we observed a high level of Phospho-PDE5A(S92), NOS3, Phospho-NOS3(S1179), and PKG1 $\beta$  in selected caveolin-rich lipid raft fractions (Figure 1F). These data demonstrate precise spatial confinement of PDE5A within plasmalemmal caveolae-rich lipid raft fractions.

### 3.2 Endothelial PDE5A reciprocally modulates NOS3 activity

To determine whether PDE5A can interact with NOS3 and reciprocally modulate its activity, we first transfected ECs with AdPDE5A. Immunoblotting confirmed a progressive increase in PDE5A expression in an MOI-dependent manner (Figure 2A).

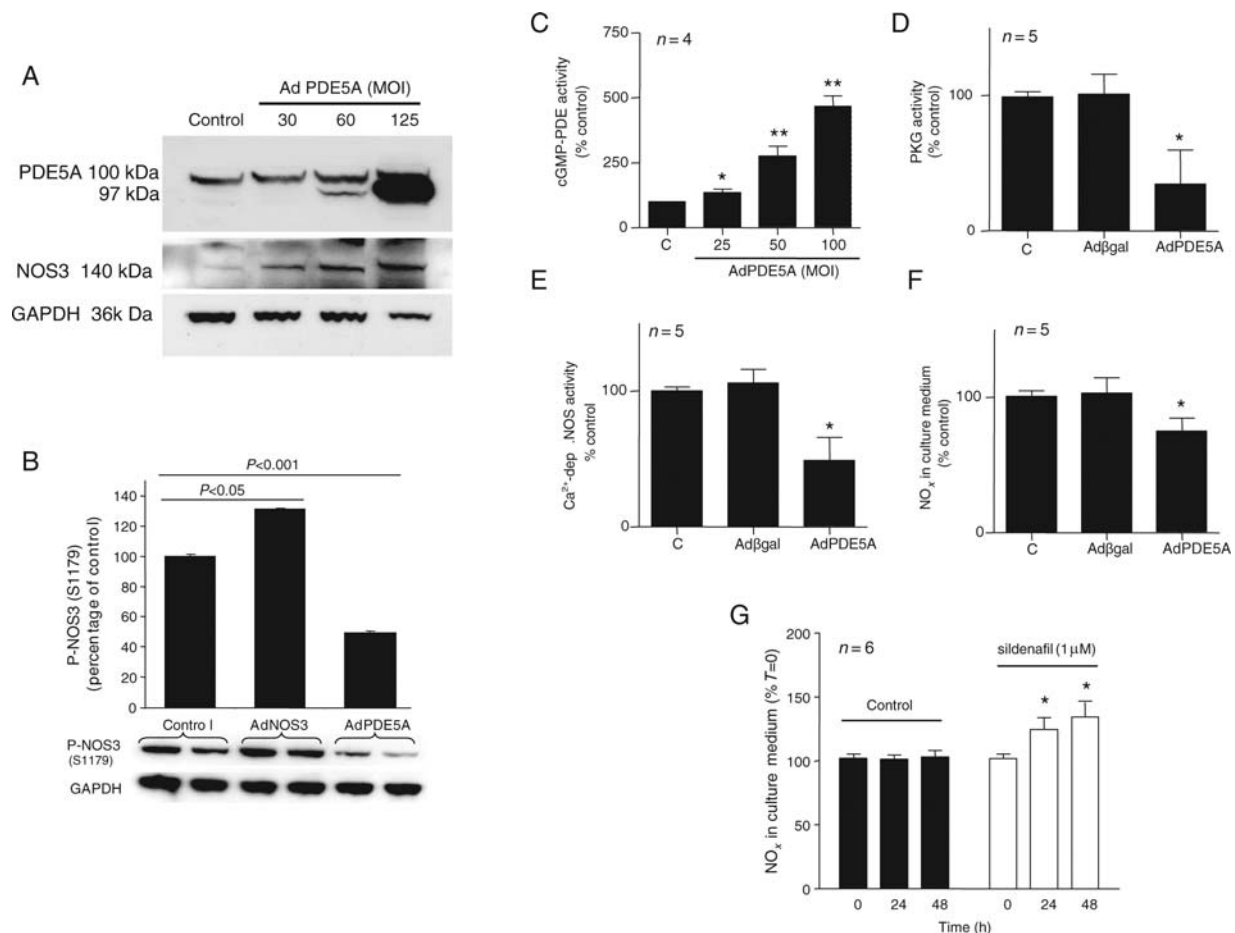


**Figure 2** Endothelial PDE5A reciprocally modulates NOS3 activity. (A) Representative immunoblot from AdPDE5A-infected BAECs at increasing MOI concentrations, probed for PDE5A and NOS3. GAPDH served as a loading control. (B) Representative immunoblot and corresponding quantification for P-NOS3(S1179) following infection of BAECs with AdNOS3 and AdPDE5A, expressed as percentage of cells transfected with Ad $\beta$ Gal ( $n = 2$ ,  $\pm$  SEM). (C) cGMP-dependent PDE activity of quiescent MPAECs infected with AdPDE5A at various MOIs, as indicated. (D) PKG activity, (E) calcium-dependent radiolabelled NOS activity, and (F) NO<sub>2</sub>/NO<sub>3</sub> (NO<sub>x</sub>) accumulation in culture medium from the MPAEC infected with AdPDE5A (MOI 50) or Ad $\beta$ gal, as indicated. Data (C–F) are expressed as percentage of control (C) (\* $P < 0.05$ , \*\* $P < 0.001$ ,  $n = 4–5$ ,  $\pm$  SEM). (G) Cells were kept in culture in the presence of PDE5A inhibitor or vehicle control for 24 and 48 h and NOS3 activity was measured by NO<sub>x</sub> production in culture medium ( $n = 6$ , \* $P < 0.05$ ,  $\pm$  SEM).

The fact that AdPDE5A leads to a parallel increase in total NOS3 expression raised the possibility that NOS3 activity might also be under PDE5A modulation. We found a significant 50% reduction in NOS3 phosphorylation at S1179 following adenoviral PDE5A overexpression ( $P < 0.001$ ); cells transfected with AdNOS3 served as a positive control giving a 30% increase in P-NOS3(S1179), when compared with cells transfected with Ad $\beta$ gal (Figure 2B;  $P < 0.05$ ).

In next series of experiments, we tested the role of endothelial PDE5A overexpression on several indices of NOS3 activity. We used quiescent MPAECs infected with AdPDE5A at MOI 50 that resulted in three- to five-fold increase in PDE5A protein expression and a 25% increase in total cGMP-dependent PDE activity (Figure 2C). Under these conditions, endothelial PKG activity decreased by about 60% (Figure 2D), whereas the conversion of [ $^3$ H]arginine-to-[ $^3$ H]citrulline and accumulation of NO<sub>x</sub> in culture medium decreased by 50% (Figure 2E) and 25% (Figure 2F), respectively. We then determined the role of PDE5 inhibitors on NOS3 activity under basal conditions. Treatment with sildenafil for 48 h resulted in a significant 20% increase in NO<sub>x</sub> in culture medium (Figure 2G;  $P < 0.05$ ) and about 15% increase in NOS3 activity by DAF2 fluorescence (data not shown), when compared with control to which vehicle was added accordingly. These data demonstrate that endothelial PDE5A can reciprocally regulate NOS3 activity.

### 3.3 Modulation of NOS3 activity occurs via endothelial PKG1

As mentioned earlier, overexpression of PDE5A downregulated PKG1 activity (Figure 2D). This led us to a hypothesis that perhaps the mechanism responsible for reciprocal interactions between NOS3 and PDE5A might occur via PKG1 signalling pathway. To test this, we first transfected MPAECs with dsRed-AdPKG1 $\alpha$  for 48 h. Figure 3A compares typical phenotypic changes in endoplasmic structure of dsRed-AdPKG1 $\alpha$ -transfected cells with reporter virus. Protein activity assay revealed a statistically significant four-fold increase in PKG activity following transfection of ECs with AdPKG1 $\alpha$ , when compared with the reporter virus or untransfected cells (Figure 3B,  $P < 0.001$ ). PKG activity in ECs transfected with Ad $\beta$ gal is lower than that in quiescent cells, but statistically insignificant ( $P = 0.0668$ ; two-tailed *t*-test). Immunoblotting confirmed that 48 h infection with dsRed-AdPKG1 $\alpha$  induced NOS3 phosphorylation at S1177 in human ECs (Figure 3C). As expected, PKG1 overexpression resulted in a significant 15% increase in NO<sub>x</sub> in culture medium (Figure 3D;  $P < 0.05$ ) and about 35% increase in NOS3 activity by DAF2 fluorescence (Figure 3E;  $P < 0.05$ ), when compared with cells transfected with Ad $\beta$ gal alone. We next tested the role of PKG1 inhibition in modulating NOS3 activity. We successfully used an siRNA strategy to generate a population of bovine endothelial PKG1 $\alpha$  $\beta$  'knockdown'. Densitometry analysis confirmed a 50% decrease in PKG1 $\beta$  protein expression following infection of BAECs with 25 nM siRNA, in the absence or presence of 8Br-cGMP (Figure 4A). 8Br-cGMP alone served

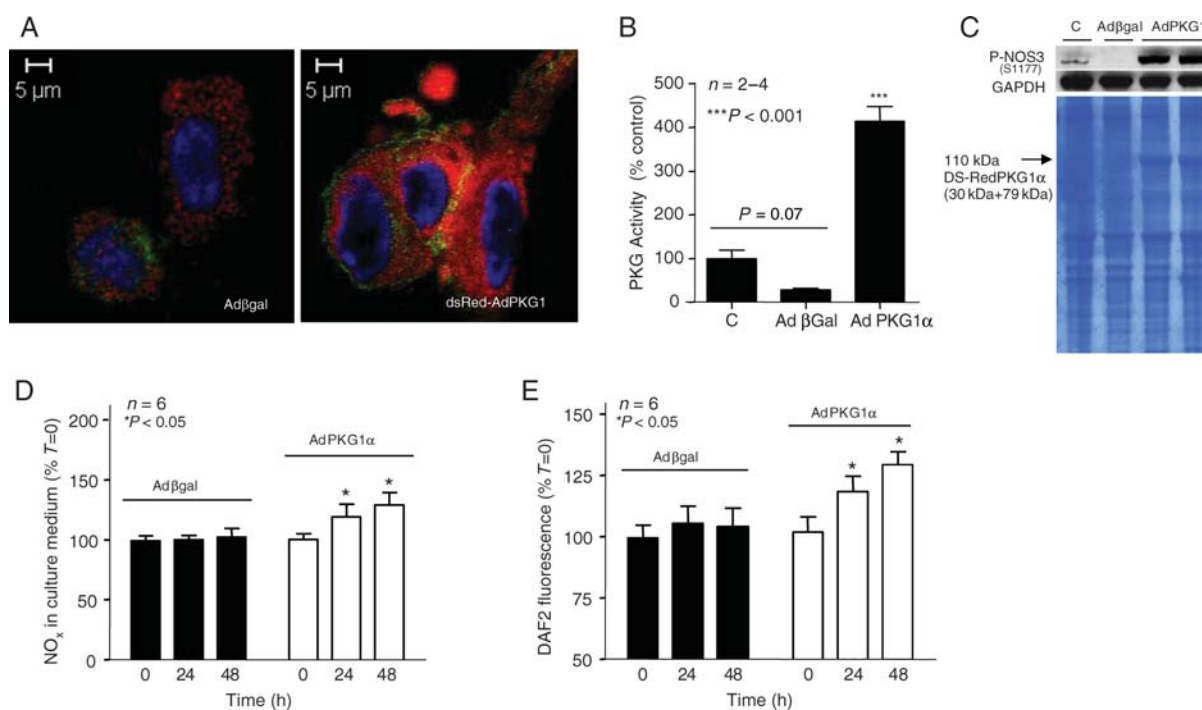


**Figure 3** Endothelial PKG1 upregulation directly regulates NOS3 activity. (A) Representative confocal micrographs of HPAECs infected with either Ad $\beta$ gal or dsRed-AdPKG1 $\alpha$  for 48 h ( $\times 100$ ); PKG1 Ab is tagged with Alexa red (left inset), and NOS3 Ab is tagged with Alexa green. PKG activity was significantly higher in dsRed-AdPKG1 $\alpha$  group, compared with quiescent or Ad $\beta$ gal transfected cells (B), expressed as percentages of untransfected cells ( $n = 2-4$ ,  $***P < 0.001$ ,  $\pm$  SEM). (C) Representative immunoblot of P-NOS3(S1177) in untransfected HPAECs (C), following infection with either Ad $\beta$ gal or dsRed-AdPKG1 $\alpha$  at 48 h (SDS gel stained with Coomassie blue). NOS3 activity was also measured in MPAECs infected with AdPKG1 for 24 and 48 h using MOI of 40, or Ad $\beta$ gal, by NO<sub>x</sub> accumulation in culture medium (D) or using DAF2 fluorescence (E). Data (A and B) are expressed as percentages of untransfected cells ( $n = 6$ ,  $*P < 0.05$ ,  $\pm$  SEM).

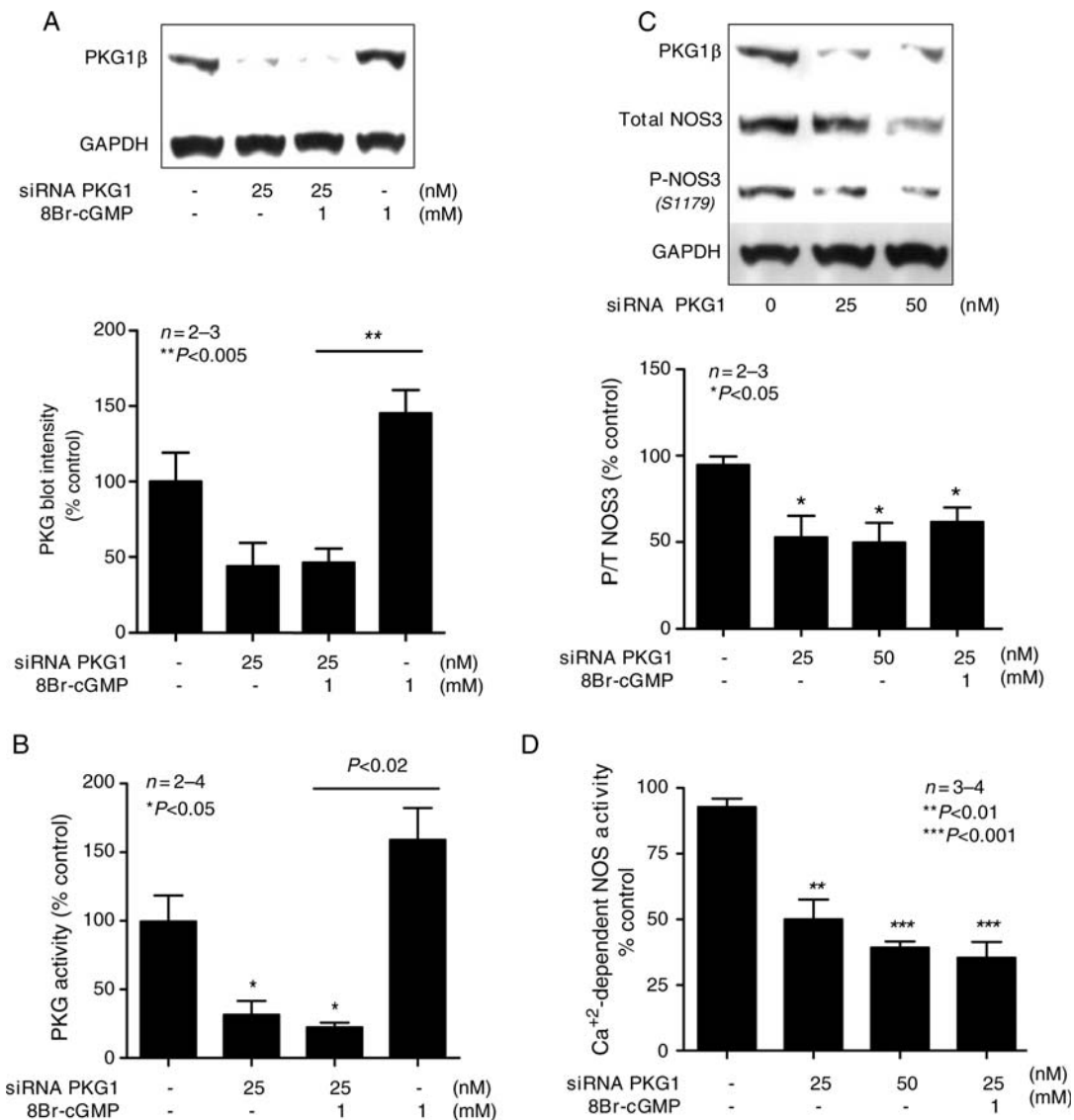


**Figure 4** Endothelial PKG1 downregulation directly regulates NOS3 activity. Data were performed using BAECs and are expressed as percentage of untransfected cells. (A) Representative immunoblot probed for PKG1 $\beta$  Ab following infection with PKG-siRNA, with corresponding densitometry quantification, in the absence or presence of 8Br-cGMP. (B) PKG activity following EC transfection with PKG1-siRNA, in the absence or presence of 8Br-cGMP. (C) Immunoblot probed for PKG1 $\beta$ , P-NOS3(S1179), and total NOS3 following infection with siRNA for PKG1 and corresponding blot quantification P/Total-NOS. (D) Calcium-dependent radiolabelled NOS activity following transfection with siRNA for PKG1 in the absence or presence of 8Br-cGMP.

as a positive control and increased PKG1 protein expression by two-fold ( $P < 0.005$ ). About 70% decrease in PKG activity was observed following transfection with siRNA, in the absence or presence of 8Br-cGMP (Figure 4B,  $P < 0.05$ ). Under these conditions, the ratio of phosphorylated/total NOS3 (P/T-NOS3) decreased by almost 50% (Figure 4C;  $P < 0.05$ ) and calcium-dependent conversion of [<sup>14</sup>C]arginine to citrulline decreased by 50–65% (Figure 4D;  $P < 0.01$ – $0.0001$ ) confirming, again, a direct role of PKG1 in NO production.

### 3.4 PDE5A has a significant physiologic impact on vascular endothelium and pulmonary circulation

On the basis of the PDE5A and NOS3 caveolar compartmentalization, we hypothesized that PDE5A can regulate vascular tone

through modulation of endothelial NO synthase activity. To determine physiological impact of endothelial PDE5A on pulmonary endothelial function, we used a mouse model for *in vivo* gene transfer technique of an adenovirus expressing PDE5A driven by a Tie2 promoter. This allowed us to overexpress PDE5A directly into PA endothelium (Figure 5A). Selective EC transfection was confirmed using PECAM beads, as well as western blotting for vWF and Tie2 (data not shown). AdGFP-PDE5A-transfected vascular rings showed over two-fold increase in cGMP-dependent PDE activity and concomitant 40% decrease in NOS3 activity (data not shown). Western blotting of isolated pulmonary ECs further confirmed that our transfection was specific to vascular endothelium (Figure 5B). When we isolated pulmonary arterial segments and used myography chamber to track changes in luminal diameter, vascular rings transfected with Ad $\beta$ gal showed a significantly greater flow-mediated vasodilation than

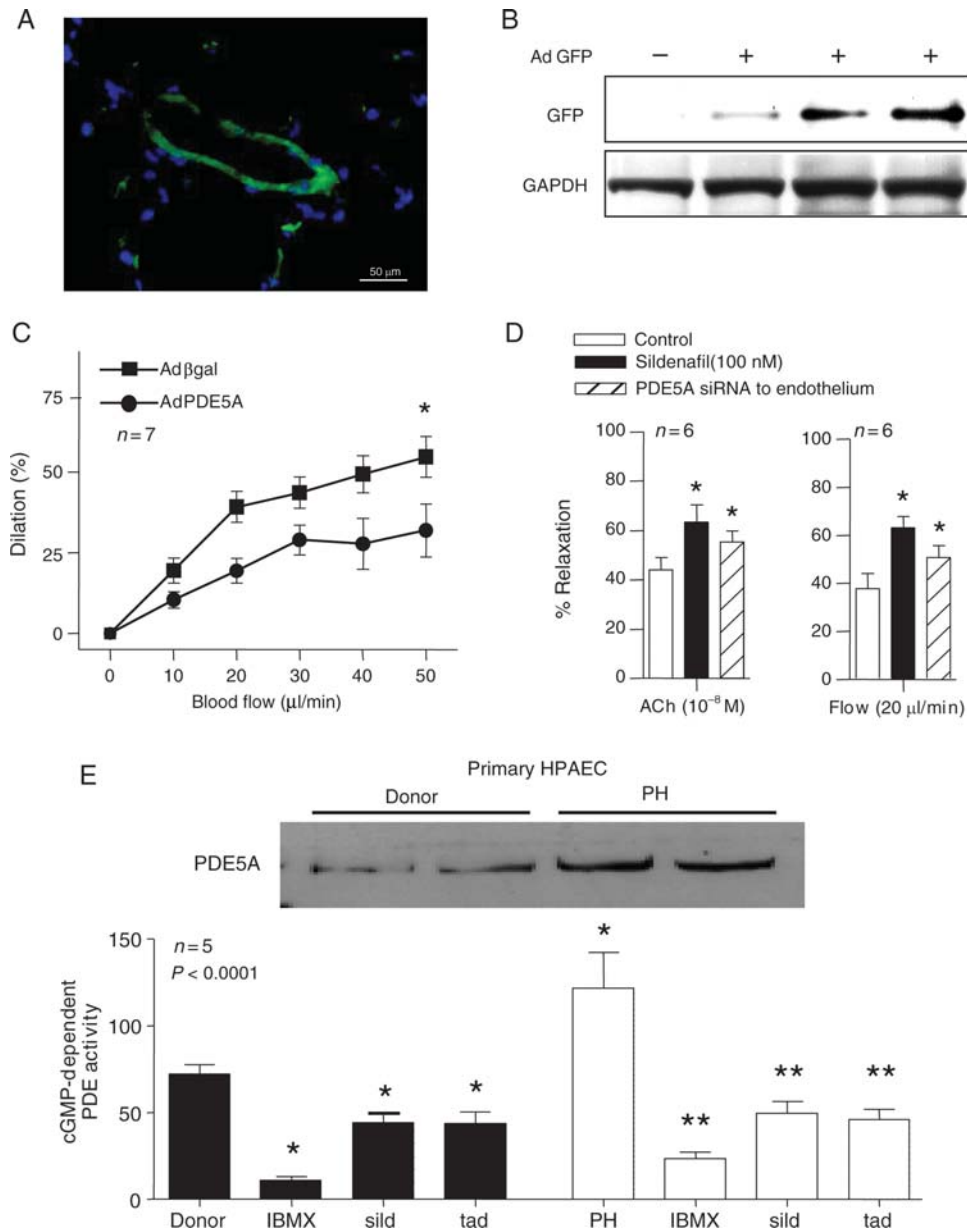


**Figure 5** A significant physiologic impact of PDE5A on vascular endothelium and pulmonary circulation. Data from selectively transfected *in vivo* mouse pulmonary rings with Tie2-PDE5A (green on inset (A)) vs. Ad $\beta\text{gal}$  control, using GFP reporter construct. (B) Representative immunoblot from vascular rings described in (A), probed for GFP in triplicate. (C) A percentage of luminal diameter-flow relationship from isolated main pulmonary arterial segments (\* $P < 0.05$ ,  $n = 7$ ,  $\pm$  SEM). (D) Relaxation of pulmonary vascular segment to acetylcholine (ACh)  $10^{-8}$  M or flow (20  $\mu\text{L}/\text{min}$ ), in the presence or absence of sild for 24 h after endothelial transfection of siRNA against PDE5A (\* $P < 0.05$  compared with control,  $n = 6$ ,  $\pm$  SEM). (E) Representative immunoblots for PDE5A in primary HPAECs isolated from patients with PH vs. heart transplant donors and corresponding cGMP-dependent PDE activity, in the presence of PDE5A inhibitors, as indicated (\* $P < 0.05$ , \*\* $P < 0.001$ ,  $n = 5$ ,  $\pm$  SEM).

PDE5A transfected vessels (Figure 5C, black squares;  $P < 0.05$ ). As represented by a curve with black circles in Figure 5C, this response was significantly blunted in the setting of adenoviral GFP-AdPDE5. After 5 days post-transfection, we performed *in vivo* pressure-flow relationship measurements in paced animals. Any given increase in mean pulmonary artery pressure in mice selectively transfected with AdGFP-PDE5A caused a significant ( $P < 0.05$ ) shift of the curve to the right that was similar to animals pre-treated with NOS inhibitor, L-NAME, for 1 week (data not shown); on the other hand, selective

overexpression of NOS3 to the endothelium caused a shift of the curve to the left (data not shown). We also observed that in the presence of sildenafil, vascular rings were significantly more susceptible to both flow- and acetylcholine-mediated vasodilation (Figure 5D,  $P < 0.05$ ). Moreover, when mouse pulmonary vascular endothelium was selectively transfected with siRNA to the endothelium, there was a significant enhancement of Ach- and flow-mediated vasodilation (Figure 5D,  $P < 0.05$ ).<sup>23</sup> These data not only provide evidence that reduction in flow-dependent vasodilation is related to the balance



between endothelial PDE5A and NO production, but also supports our previous findings on ECs in culture (Figure 2).

### 3.5 PDE5A is highly upregulated in pulmonary endothelium isolated from patients with pulmonary hypertension

A number of clinical studies have reported the beneficial effect of PDE5A inhibition in the treatment of primary pulmonary hypertension (PH).<sup>24–27</sup> Although it is believed that beneficial effect is due to inhibition of PDE5A derived from pulmonary vascular SMCs, we hypothesized that pulmonary ECs also contribute in this process. To test this hypothesis, we isolated pulmonary ECs from patients with known PH and healthy donors. As expected, a significant increase in PDE5A expression and activity was detected in ECs isolated from patients with PH (Figure 5E). In addition, more than 60% inhibition of total cGMP-dependent PDE activity was observed in the presence of sildenafil and tadalafil (1  $\mu$ M) in pulmonary ECs from patients with PH ( $P < 0.0001$ ). Although a considerable inhibition of cGMP-dependent PDE activity was also seen in donor ECs treated with PDE5 inhibitors, the differences were not statistically significant when compared with quiescent donor cells.

## 4. Discussion

The importance of SMC-derived PDE5A in regulation of vascular tone is widely accepted. Although few reports suggest the presence of PDE5A in vascular endothelium, location of endothelial PDE5A, or its functional role, has not yet been characterized. Ashikaga *et al.*<sup>5</sup> reported that PDE5A is expressed in cultured BAECs, whereas Nethererton and Maurice<sup>4</sup> found PDE5A in other EC types, including human microvascular ECs. Zhu *et al.*<sup>3</sup> noted that in pulmonary microvascular ECs, activation of particulate guanyl cyclase by atrial natriuretic peptide and inhibition of PDE5A by zaprinast reduced growth and induced apoptosis.

The major finding from our study is that we provide an exact localization of PDE5A within vascular ECs. This is also the first study to report a role of endothelial PDE5A and PKG1 in regulation of vascular tone through modulation of NO production.

A growing body of literature suggests that the basic machinery for the NO/cGMP/PKG signalling pathway is present within caveolin-rich lipid rafts. Others have shown that NOS3,<sup>7,8</sup> sGC, PKG, and PKA<sup>9,10</sup> are at or near caveolae. Caveolae represent a plasma membrane subdomain enriched with cholesterol, glycosphingolipids, and structural proteins and have been intensively studied as domains for the

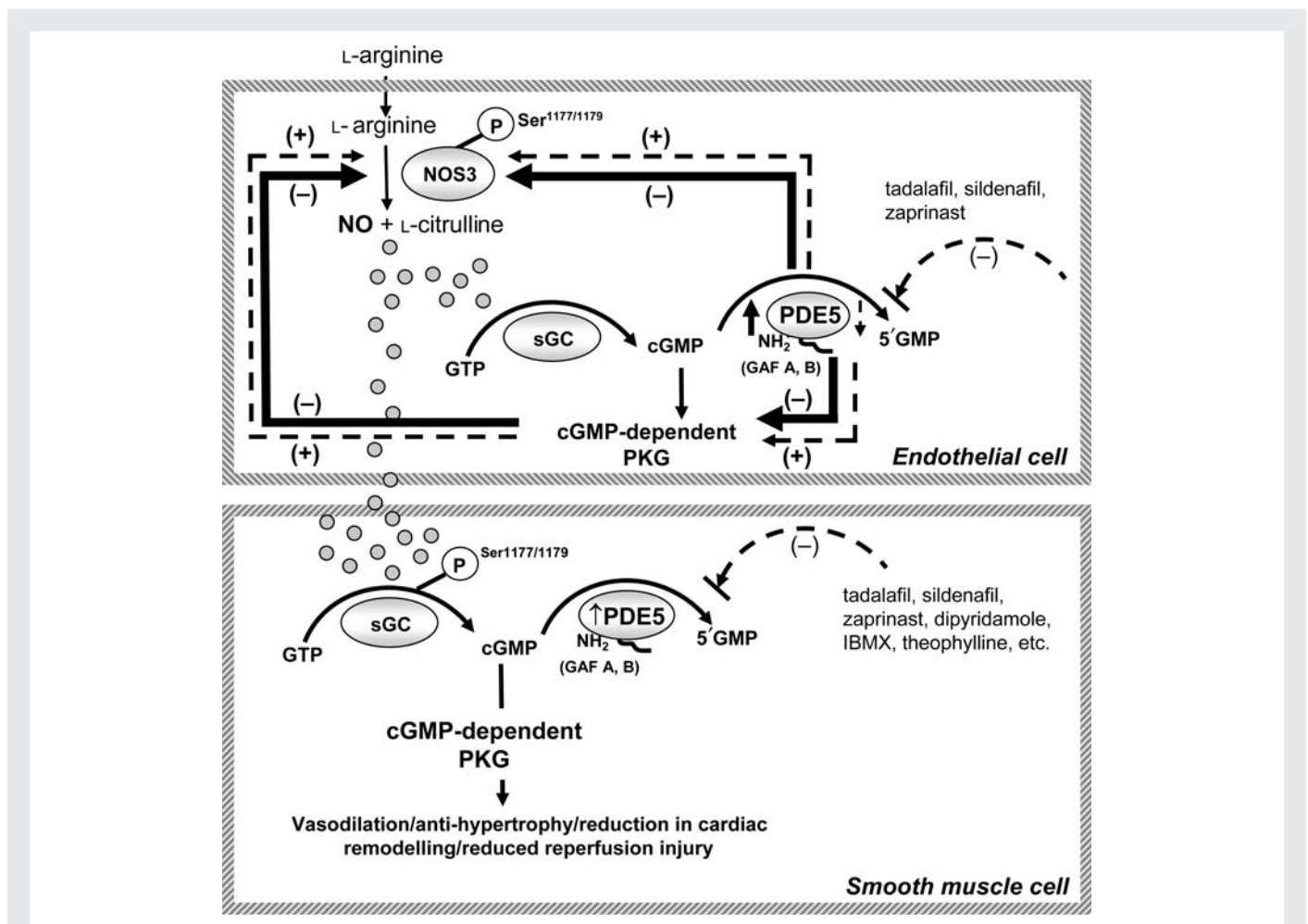


**Figure 6** Schematic representation of reciprocal feedback loop between endothelial PDE5A, NOS3, and PKG1. Overexpression of endothelial PDE5A results in a reciprocal reduction in NOS3 activity and phospho-NOS3 expression. Concomitantly, a significant decrease in PKG1 activity occurs and further potentiates vascular dysfunction. These processes can be reversed by either PDE5A inhibitors or PKG1 overexpression.

compartmentalization of plasma membrane-linked signal transduction pathways. The fact that we found PDE5A to be also localized within the caveolae, not only provides a novel concept of a traditional NO/cGMP/PDE5A signalling pathway, but also underlines the fundamentally important role of PDE5A and cGMP in the molecular mechanism of endothelium-mediated vasorelaxation, especially in conditions leading to endothelial dysfunction. A double band pattern of bovine PDE5A during western blotting (Figures 1A and 2A) had been previously reported in other ECs<sup>4</sup> and SMCs<sup>28,29</sup> and requires further investigation. This could possibly be explained by an enhancement of one of the PDE5 isoforms (A1, A2, or A3) during protein overexpression with AdPDE5A which are usually very difficult to separate on western blotting due to a similar molecular size.<sup>30</sup> On the other hand, it might correspond to the phosphorylated, higher-moiety and unphosphorylated, lower-moiety forms.

Our data demonstrate that modulation of endothelial PDE5A activity results in reciprocal changes in NOS3 activity (see Figure 6). Under basal conditions, treatment of human endothelium with PDE5A inhibitors resulted in a significant increase in NOS3 activity and phosphorylation, whereas overexpression of PDE5A using an adenoviral vector or PH model, both *in vivo* and in cell culture, resulted in a reciprocal reduction in NOS3 activity and endothelium-dependent vasodilation. Interestingly, under these conditions, total NOS3 expression is upregulated. In addition, we found that PDE5A overexpression leads to a significant decrease in PKG1 activity. The role of PKG in NOS phosphorylation has not been well studied in the literature. Butt *et al.*<sup>31</sup> found that purified recombinant endothelial NOS3 can be strongly phosphorylated by PKG2, whereas PKG1 showed much less <sup>32</sup>P incorporation into the enzyme. The fact that PKG1 overexpression with adenoviral vector leads to a 35% increase in NOS3 activity and rapid NOS3 phosphorylation at S1177 in human EC indicates reciprocal and direct interplay between NOS3 and PKG. A significant decrease in both phosphorylated to total NOS3 ratio and calcium-dependent NOS activity following transfection of ECs with PKG-siRNA further supports this finding. The fact that we observed a significant and flow-dependent vasodilation in pulmonary vascular rings selectively transfected with Adβgal, but not with AdPDE5A, together with our *in vivo* data strongly suggests that reduction in flow-mediated vasodilation is related, at least in part, to PDE5A and depletion in NO production. A similar effect was obtained in animals pre-treated with L-NAME. We also observed that in the presence of either sildenafil or PDE5-siRNA, vascular rings were significantly more susceptible to both acetylcholine- and flow-mediated vasodilation. In addition, a significant decrease in total cGMP-dependent PDE activity was observed in pulmonary ECs harvested from patients with PH in the presence of PDE5 inhibitors, again, further supporting a key role of PDE5A in pathology of the disease. Collectively, these data suggest a strong relationship between endothelial PDE5A and PKG1 that may contribute to modulation of NO production, independent of SMCs.

#### 4.1 Mechanisms

The proposed molecular mechanisms responsible for the regulation of endothelial-dependent vascular tone appear to involve direct reciprocal interactions between endothelial PDE5A, NOS3, and PKG. We studied the role of Akt in this process; however, we did not observe any statistically significant differences in expression or activity of P-Akt(S473) (data not shown).

In summary, we demonstrate primary location of PDE5A at or near caveolae in vascular ECs. The spatial localization of PDE5A at the level of caveolin-rich lipid rafts allows for a feedback loop between endothelial PDE5A and NOS3 via cGMP-dependent second messenger. This study reveals several new points helping to elucidate the nature of endothelial PDE5A and its regulation of NO production and vascular tone. Further research on the involvement of PDE5A in PH, diabetes, atherosclerosis, erectile dysfunction, as well as inflammation, angiogenesis, and tumour formation is needed in order to help better understand the importance and involvement of PDE5A in our physiology as well as to provide new and exciting therapeutic options in the future.

#### Acknowledgements

The authors thank David A. Kass, M.D., and Manling Zang, M.D., from Division of Cardiology, Department of Medicine, Johns Hopkins Medical Institutions, for their expert opinion and providing dsRed-AdPKG1α.

**Conflict of interest:** none declared.

#### Funding

This work was supported, in part, by the Bernard A. and Rebecca S. Bernard Foundation, a scientist development grant from the American Heart Association, the WW Smith Foundation, and the NIH grant 7 F32 HL-82132-02. H.C.C. receives research support from the Vascular Medicine Institute, the Institute for Transfusion Medicine, and the Hemophilia Center of Western Pennsylvania.

#### References

- Feil R, Lohmann SM, de Jonge H, Walter U, Hofmann F. Cyclic GMP-dependent protein kinases and the cardiovascular system: insights from genetically modified mice. *Circ Res* 2003;**93**:907–916.
- Takimoto E, Champion HC, Li M, Belardi D, Ren S, Rodriguez ER *et al.* Chronic inhibition of cyclic GMP phosphodiesterase 5A prevents and reverses cardiac hypertrophy. *Nat Med* 2005;**11**:214–222.
- Zhu B, Strada S, Stevens T. Cyclic GMP-specific phosphodiesterase 5 regulates growth and apoptosis in pulmonary endothelial cells. *Am J Physiol Lung Cell Mol Physiol* 2005;**289**:L196–L206.
- Netherton SJ, Maurice DH. Vascular endothelial cell cyclic nucleotide phosphodiesterases and regulated cell migration: implications in angiogenesis. *Mol Pharmacol* 2005;**67**:263–272.
- Ashikaga T, Strada SJ, Thompson WJ. Altered expression of cyclic nucleotide phosphodiesterase isozymes during culture of aortic endothelial cells. *Biochem Pharmacol* 1997;**54**:1071–1079.
- Pfeifer A, Ruth P, Dostmann W, Sausbier M, Klatt P, Hofmann F. Structure and function of cGMP-dependent protein kinases. *Rev Physiol Biochem Pharmacol* 1999;**135**:105–149.
- Feron O, Belhassen L, Kobzik L, Smith TW, Kelly RA, Michel T. Endothelial nitric oxide synthase targeting to caveolae: specific interactions with caveolin isoforms in cardiac myocytes and endothelial cells. *J Biol Chem* 1996;**271**:22810–22814.
- Garcia-Cardena G, Oh P, Liu J, Schnitzer JE, Sessa WC. Targeting of nitric oxide synthase to endothelial cell caveolae via palmitoylation: implications for nitric oxide signaling. *Proc Natl Acad Sci USA* 1996;**93**:6448–6453.
- Linder AE, McCluskey LP, Cole KR III, Lanning KM, Webb RC. Dynamic association of nitric oxide downstream signaling molecules with endothelial caveolin-1 in rat aorta. *J Pharmacol Exp Ther* 2005;**314**:9–15.
- MacMillan-Crow LA, Murphy-Ullrich JE, Lincoln TM. Identification and possible localization of cGMP-dependent protein kinase in bovine aortic endothelial cells. *Biochem Biophys Res Commun* 1994;**201**:531–537.
- Antonov AS, Nikolaeva MA, Klueva TS, Romanov Yu A, Babaev VR, Bystrevskaya VB *et al.* Primary culture of endothelial cells from atherosclerotic human aorta. Part 1. Identification, morphological and ultrastructural characteristics of two endothelial cell subpopulations. *Atherosclerosis* 1986;**59**:1–19.
- Li Z, Ajdic J, Eigenthaler M, Du X. A predominant role for cAMP-dependent protein kinase in the cGMP-induced phosphorylation of vasodilator-stimulated phosphoprotein and platelet inhibition in humans. *Blood* 2003;**101**:4423–4429.
- Saalbach A, Aust G, Hausteiner UF, Herrmann K, Anderegg U. The fibroblast-specific MAb AS02: a novel tool for detection and elimination of human fibroblasts. *Cell Tissue Res* 1997;**290**:593–599.

14. Campbell JH, Campbell GR. Methods of growing vascular smooth muscle in culture. In: Campbell JH, Campbell GR, eds. *Vascular Smooth Muscle in Culture*. Boca Raton, FL: CRC Press; 1987.
15. Champion HC, Georgakopoulos D, Takimoto E, Isoda T, Wang Y, Kass DA. Modulation of *in vivo* cardiac function by myocyte-specific nitric oxide synthase-3. *Circ Res* 2004;**94**:657–663.
16. Stan RV. Structure and function of endothelial caveolae. *Microsc Res Tech* 2002;**57**:350–364.
17. Zhou W, Dasgupta C, Negash S, Raj JU. Modulation of pulmonary vascular smooth muscle cell phenotype in hypoxia: role of cGMP-dependent protein kinase. *Am J Physiol Lung Cell Mol Physiol* 2007;**292**:L1459–L1466.
18. Takimoto E, Champion HC, Belardi D, Moslehi J, Mongillo M, Mergia E *et al*. cGMP catabolism by phosphodiesterase 5A regulates cardiac adrenergic stimulation by NOS3-dependent mechanism. *Circ Res* 2005;**96**:100–109.
19. Takayasu KT. Immunocytochemistry on ultrathin frozen sections. *Histochem J* 1980;**12**:381–390.
20. Champion HC, Bivalacqua TJ, Toyoda K, Heistad DD, Hyman AL, Kadowitz PJ. *In vivo* gene transfer of prepro-calcitonin gene-related peptide to the lung attenuates chronic hypoxia-induced pulmonary hypertension in the mouse. *Circulation* 2000;**101**:923–930.
21. Champion HC, Georgakopoulos D, Haldar S, Wang L, Wang Y, Kass DA. Robust adenoviral and adeno-associated viral gene transfer to the *in vivo* murine heart: application to study of phospholamban physiology. *Circulation* 2003;**108**:2790–2797.
22. Mulvany MJ, Halpern W. Contractile properties of small arterial resistance vessels in spontaneously hypertensive and normotensive rats. *Circ Res* 1977;**41**:19–26.
23. Wilson A, Zhou W, Champion HC, Alber S, Tang ZL, Kennel S *et al*. Targeted delivery of oligodeoxynucleotides to mouse lung endothelial cells *in vitro* and *in vivo*. *Mol Ther* 2005;**12**:510–518.
24. Sastry BK, Narasimhan C, Reddy NK, Raju BS. Clinical efficacy of sildenafil in primary pulmonary hypertension: a randomized, placebo-controlled, double-blind, crossover study. *J Am Coll Cardiol* 2004;**43**:1149–1153.
25. Corbin JD, Beasley A, Blount MA, Francis SH. High lung PDE5: a strong basis for treating pulmonary hypertension with PDE5 inhibitors. *Biochem Biophys Res Commun* 2005;**334**:930–938.
26. Galie N, Ghofrani HA, Torbicki A, Barst RJ, Rubin LJ, Badesch D *et al*. Sildenafil citrate therapy for pulmonary arterial hypertension. *N Engl J Med* 2005;**353**:2148–2157.
27. Hemnes AR, Champion HC. Sildenafil, a PDE5 inhibitor, in the treatment of pulmonary hypertension. *Expert Rev Cardiovasc Ther* 2006;**4**:293–300.
28. Lin G, Xin ZC, Lue TF, Lin CS. Phosphodiesterase-5 isoforms: differential cyclic guanyl monophosphate binding and cyclic guanyl monophosphate catalytic activities, and inhibitory effects of sildenafil and vardenafil. *J Urol* 2006;**176**:1242–1247.
29. Pauvert O, Lugnier C, Keravis T, Marthan R, Rousseau E, Savineau JP. Effect of sildenafil on cyclic nucleotide phosphodiesterase activity, vascular tone and calcium signaling in rat pulmonary artery. *Br J Pharmacol* 2003;**139**:513–522.
30. Lin CS, Chow S, Lau A, Tu R, Lue TF. Human PDE5A gene encodes three PDE5 isoforms from two alternate promoters. *Int J Impot Res* 2002;**14**:15–24.
31. Butt E, Bernhardt M, Smolenski A, Kotsonis P, Frohlich LG, Sickmann A *et al*. Endothelial nitric-oxide synthase (type III) is activated and becomes calcium independent upon phosphorylation by cyclic nucleotide-dependent protein kinases. *J Biol Chem* 2000;**275**:5179–5187.